

Original Article

Angiotensin Type 1 Receptor Blockade Prevents Cardiac Remodeling in Mice with Pregnancy-Associated Hypertension

Akira SAKAIRI¹, Junji ISHIDA¹, Kaori HONJO¹, Saki INABA¹, Shoko NAKAMURA¹, Fumihiko SUGIYAMA², Ken-ichi YAGAMI², and Akiyoshi FUKAMIZU¹

Pregnancy-induced hypertension (PIH) is a life-threatening disorder for both mother and fetus; cardiac dysfunction is the major complication and can result in further deterioration. Recently, it has been recognized that aberrant activation of angiotensin type 1 receptor (AT1) signaling contributes to the pathogenesis of PIH, but the details of the relationship between cardiac injury and enhanced AT1 signaling in PIH are still unclear. We previously generated a transgenic mouse model of pregnancy-associated hypertension (PAH) *via* overproduction of angiotensin II, an endogenous ligand of AT1, in the maternal circulation during late pregnancy. In the present study, we administered olmesartan, an AT1 blocker, to suppress redundant AT1 signaling in PAH mice and evaluated the efficacy of this treatment in cardiac remodeling. Olmesartan treatment significantly lowered the blood pressure of PAH mice, and hypertrophy as well as increased plasma levels of cardiac injury markers were also markedly reduced. Histological analyses revealed that morphological abnormalities and fibrosis in the hearts of PAH mice recovered to the levels of normal pregnant wild-type mice after the administration of olmesartan. Moreover, in fibrotic regions of PAH hearts, olmesartan treatment significantly decreased the extent of cardiac injury and apoptosis. These results indicate that the activation of AT1 signaling pathways during maternal hypertension plays a critical role in cardiac remodeling in PAH mice, and suggest that treatment with an AT1 blocker could effectively ameliorate cardiac dysfunction during pregnancy with hypertension *in vivo*. (*Hypertens Res* 2008; 31: 2165–2175)

Key Words: cardiac remodeling, pregnancy-associated hypertension, angiotensin type 1 receptor (AT1), renin-angiotensin system (RAS), angiotensin receptor blocker (ARB)

Introduction

Hypertension complicates approximately 10% of all pregnancies and remains a major cause of both fetal and maternal morbidity and mortality. The most serious problems are associated with preeclampsia-eclampsia, a disorder peculiar to

pregnancy. Pregnancy-induced hypertension (PIH) is characterized by blood pressure elevation and proteinuria after 20 weeks of gestation in humans (*1*); the prevention of PIH would have a significant impact on maternal and neonatal outcome. However, the pathophysiology of PIH remains poorly understood. The cardiac enlargement characteristic of normal pregnancy can result in left ventricular dysfunction in

From the ¹Center for Tsukuba Advanced Research Alliance, Graduate School of Life and Environmental Sciences, University of Tsukuba, Tsukuba, Japan; and ²Institute of Basic Medical Sciences, Laboratory Animal Resource Center, University of Tsukuba, Tsukuba, Japan.

This work was supported by the following grants: The 21st Century COE Program, a Grant-in-Aid for Scientific Research (S), a Grant-in-Aid for Young Scientists (B), and a Grant-in-Aid for JSPS Fellows from the Ministry of Education, Culture, Sports, Science and Technology of Japan, and the University of Tsukuba Special Research Program.

Address for Reprints: Akiyoshi Fukamizu, Ph.D., Center for Tsukuba Advanced Research Alliance, University of Tsukuba, 1–1–1 Tennodai, Tsukuba 305–8577, Japan. E-mail: akif@tara.tsukuba.ac.jp

Received September 11, 2008; Accepted in revised form October 21, 2008.

the presence of elevated blood pressure. In chronic hypertension, increased cardiac hypertrophy and cardiac remodeling, including tissue fibrosis and myocardial injury, result in cardiac dysfunction. To our knowledge, no studies to date have investigated the pathology of cardiac remodeling and injury in PIH.

The renin-angiotensin system (RAS) is an important regulator of blood pressure, sodium, and fluid homeostasis (2, 3). In normal pregnancy, estrogen causes increased RAS activity by increasing both tissue and circulating levels of angiotensinogen (ANG) (4, 5) and renin (RN) (6–9). Consequently, plasma levels of angiotensin II (Ang II), a vasopressor octapeptide derived from ANG, are increased in association with increased ANG and plasma RN activity during gestation (10, 11). Normal pregnant women are resistant to the pressor effects of Ang II (12–14), and they remain normotensive despite a 2-fold increase in Ang II. On the other hand, vascular sensitivity to Ang II is elevated in preeclamptic women (13). The diverse actions of Ang II are mediated by several types of receptors expressed in a variety of target tissues. Two Ang II receptors have been identified in humans: AT1 (type 1) and AT2 (type 2). Rodents, on the other hand, express Ang II type 1a (AT1a) and Ang II type 1b (AT1b). In rodents, blood pressure and pathophysiological effects of RAS are primarily mediated by the AT1a receptor (15). Although the etiology and pathology of PIH remain enigmatic, it is thought that aberrantly activated AT1 signaling is one of the major causes of increased Ang II sensitivity, which causes PIH pathogenesis (16–18). However, the detailed relationship between cardiac injury and enhanced AT1 signaling in PIH remains unclear.

We previously generated mice with pregnancy-associated hypertension (PAH) by mating females expressing human angiotensinogen (hANG) with males expressing human renin (hRN) (19). In PAH mice, maternal hypertension starts from 14 d of gestation (E14) until delivery (E19–20) due to the generation of excessive angiotensin I, the precursor of Ang II, by hRN secretion from the fetus into the maternal circulation (19, 20). Systolic blood pressure (SBP) at E19 in PAH dams reaches 160 mmHg but remains around 100 mmHg in normal pregnant mice. In addition to hypertension, PAH dams show cardiac hypertrophy and proteinuria and frequently display convulsions. At-term fetuses in PAH pregnancies show severe intrauterine growth retardation (IUGR), and the mean body weight of PAH fetuses at E19 is about 65% of that of wild-type (WT) fetuses (20–22). We have previously demonstrated the importance of the AT1 receptor on PIH pathogenesis using PAH mice (20). Genetic disruption of the AT1 receptor in PAH dams and short-term administration of an angiotensin receptor blocker (ARB) greatly improved the pathology of PAH mice, including hypertension and cardiac hypertrophy (20). In the present study, we administered the ARB olmesartan during late pregnancy to suppress the redundant AT1 signaling in PAH mice and evaluated the efficacy of this drug on cardiac remodeling. The treatment of PAH

mice using olmesartan resulted in remarkable improvement in cardiac hypertrophy, the plasma level of cardiac injury marker, cardiac fibrosis, and damage to cardiomyocytes. These results indicated that the activated-AT1 signaling played a critical role in cardiac remodeling in pregnancy-associated hypertension.

Methods

Animals

As described previously, PAH mice were generated by mating females expressing hANG with males expressing hRN (19). Animal experiments were carried out in a humane manner under approval from the Institutional Animal Experiment Committee of the University of Tsukuba. Experiments were performed in accordance with the Regulation of Animal Experiments of the University of Tsukuba and the Fundamental Guidelines for Proper Conduct of Animal Experiments and Related Activities in Academic Research Institutions under the jurisdiction of the Ministry of Education, Culture, Sports, Science and Technology. Transgenic mice and age-matched WT mice (C57BL/6J) at 8–16 weeks of age were used for cross-mating.

Administration of ARB

Olmesartan, an ARB, was a gift from Daiichi Sankyo Co., Ltd. (Tokyo, Japan). Olmesartan was dissolved in sterile water containing 0.01% NaHCO₃ and 0.01% KHCO₃ and administered at a dose of 3 mg/kg/d in drinking water from E13 to E19. This dosage was determined by preliminary experiments to bring the SBP of PAH mice to within 90–120 mmHg. Female mice were classified into four groups: 1) non-treated WT, 2) olmesartan-treated WT, 3) non-treated PAH, and 4) olmesartan-treated PAH.

Measurement of Blood Pressure and Body Weight

SBP was measured in awake animals (each group, $n=11$) using a non-invasive computerized tail-cuff blood pressure system (BP-98a, Softron, Tokyo, Japan) as described previously (19, 20, 23). During measurement, unanesthetized mice were guided into a holder mounted on a thermostatically controlled warming plate and maintained at 37°C. Body weight was measured on E1 and from E9 to E19 (each group, $n=11$).

Plasma Creatine Kinase and Creatine Kinase MB Assay

Female mice were anesthetized with diethyl ether on day 19 of gestation. Blood samples were collected from the inferior vena cava into ice-cold tubes containing heparin and immedi-

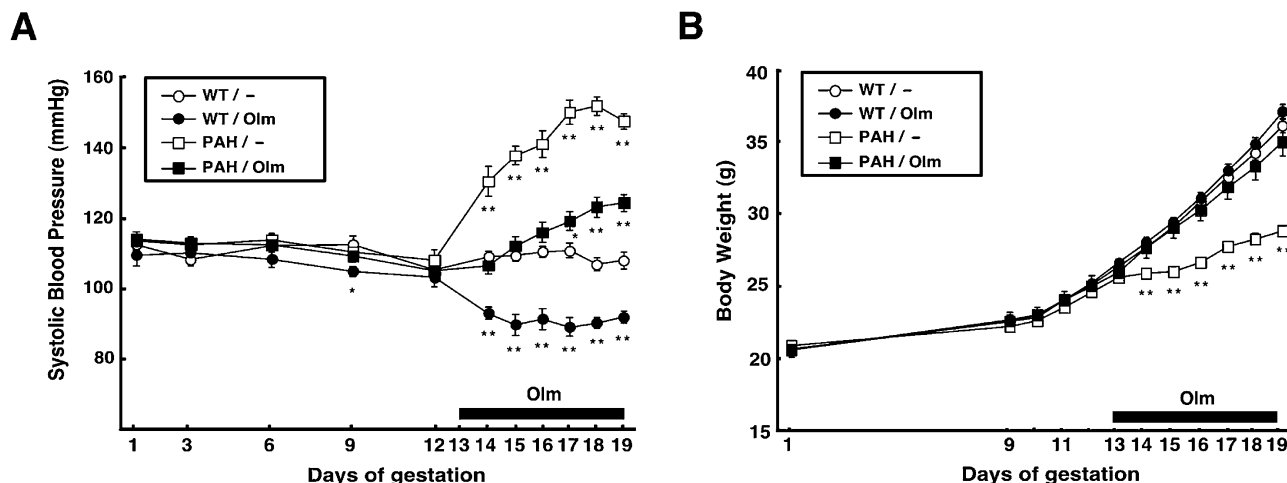


Fig. 1. Amelioration of hypertension and normalization of weight gain in PAH mice by olmesartan treatment. *A:* Systolic blood pressure during pregnancy in non-treated WT mice ($n=11$), olmesartan-treated WT mice ($n=11$), non-treated PAH mice ($n=11$), and olmesartan-treated PAH mice ($n=11$). * $p < 0.05$ vs. non-treated WT mice, ** $p < 0.001$ vs. non-treated WT mice. *B:* Changes in maternal body weight during pregnancy of non-treated WT mice ($n=11$), olmesartan-treated WT mice ($n=11$), non-treated PAH mice ($n=11$), and olmesartan-treated PAH mice ($n=11$). ** $p < 0.001$ vs. non-treated WT mice.

ately centrifuged. After centrifugation, the supernatant as the plasma fraction was stored at -80°C until needed. To assess myocardial injury, plasma levels of creatine kinase (CK) and creatine kinase MB (CKMB) in female mice (each group, $n=4-5$) were assayed using a Fuji Dri-Chem 3500 V device (Fuji Film Medical Co., Ltd., Tokyo, Japan).

Histological Analysis

Female mice were euthanized on day 19 of gestation. Their hearts were immediately excised and fixed with 4% paraformaldehyde in 0.1 mol/L phosphate buffer (pH 7.2) (each group, $n=3$). After being sufficiently washed in PBS, tissues were dehydrated and embedded in paraffin wax. Sections were cut to $5\ \mu\text{m}$ thickness using a rotary microtome (Microm HM340E, Walldorf, Germany). For morphological observation, sections were stained with hematoxylin and eosin. To evaluate cardiac fibrosis, sections were also stained with Masson's trichrome. To determine myocardial damage, we detected cardiac iron accumulation by Prussian blue staining. Stained sections were examined using a Leica DMR/XA fluorescence microscope (Fototequipment: Leica DC 300F; Leica, Wetzlar, Germany) and a Leica MZ LFIII fluorescence stereomicroscope (Leica). To evaluate the average cardiomyocyte diameter in the left ventricle, the shortest diameter of each cardiomyocyte was measured in nucleated transverse sections. Two hundred cardiomyocytes per specimen were measured using Win Roof software (Mitani Co., Ltd., Fukui, Japan).

TUNEL (Terminal Deoxynucleotide Transferase-Mediated dUTP Nick End Labeling) Assay

To detect apoptotic cells, TUNEL assay was performed on paraffin-embedded heart sections of pregnant mice after 19 d of gestation (each group, $n=3$) using the *in situ* Cell Death Detection Kit (Roche Diagnostics GmbH, Mannheim, Germany) according to the manufacturer's instructions. For nuclear counterstaining, sections were subsequently stained with Hoechst 33258. The percentage of TUNEL-positive cells in 12 randomly chosen left ventricular wall sections was determined using Win Roof software (Mitani Co., Ltd.). Fluorescence was visualized on a Leica DMR/XA fluorescence microscope (Fototequipment: Leica DC 300F; Leica).

Statistical Analysis

Results are expressed as the mean \pm SEM. For two independent samples, statistical comparison was performed using Student's *t*-test, Welch's *t*-test, or the Mann-Whitney *U* test as appropriate. $p < 0.05$ was considered statistically significant.

Results

Olmesartan Treatment of PAH Mice

First, we examined the effectiveness of olmesartan treatment on PAH pathology in pregnant dams. The SBP remained unchanged during pregnancy in non-treated WT dams (Fig. 1A, opened circle), but began to increase in PAH dams from 14 d of gestation (E14), reaching a peak on the 18th day of

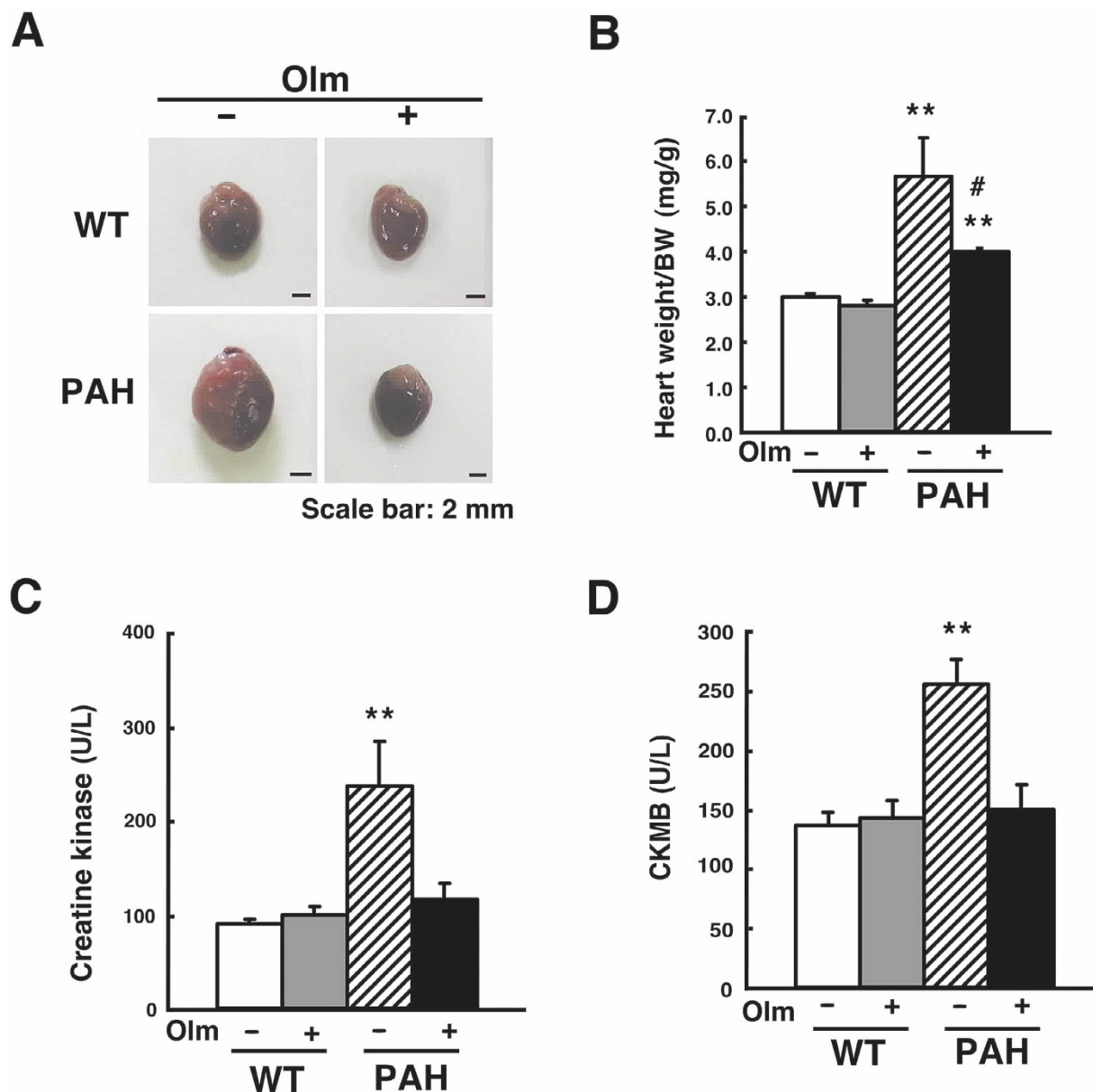


Fig. 2. Evaluation of cardiac hypertrophy and plasma levels of myocardial injury markers. *A:* Gross observation of the heart on day 19 of gestation. Scale bar is 2 mm. *B:* The ratio of heart weight to body weight (BW) in pregnant mice at 19 d of gestation ($n=6$). Each heart weight is represented by wet weight. ** $p < 0.001$ vs. non-treated WT mice, # $p < 0.05$ vs. non-treated PAH mice. *C:* Plasma levels of creatine kinase in pregnant mice at 19 d of gestation ($n=4-5$). ** $p < 0.01$ vs. non-treated WT mice. *D:* Plasma levels of isoenzyme of creatine kinase (CKMB) in pregnant mice at 19 d of gestation ($n=4-5$). ** $p < 0.01$ vs. non-treated WT mice.

gestation (E18) (Fig. 1A, opened square). Therefore, we administered olmesartan to PAH dams from E13 to E19. Olmesartan significantly lowered the blood pressure of PAH mice to the normal range, except for a slight elevation observed on E18 and E19 (Fig. 1A, closed square). The blood pressure of olmesartan-treated WT mice was significantly lower than that of non-treated WT mice during treatment, but was within the normal range (Fig. 1A, closed circle). PAH

dams displayed a significant suppression of weight gain during late pregnancy in comparison with non-treated and olmesartan-treated WT dams. However, the weight gain of olmesartan-treated PAH dams was similar to that of non-treated and olmesartan-treated WT dams (Fig. 1B). These findings indicate that AT1 blockade by olmesartan treatment can effectively reduce blood pressure and normalize weight gain in PAH mice.

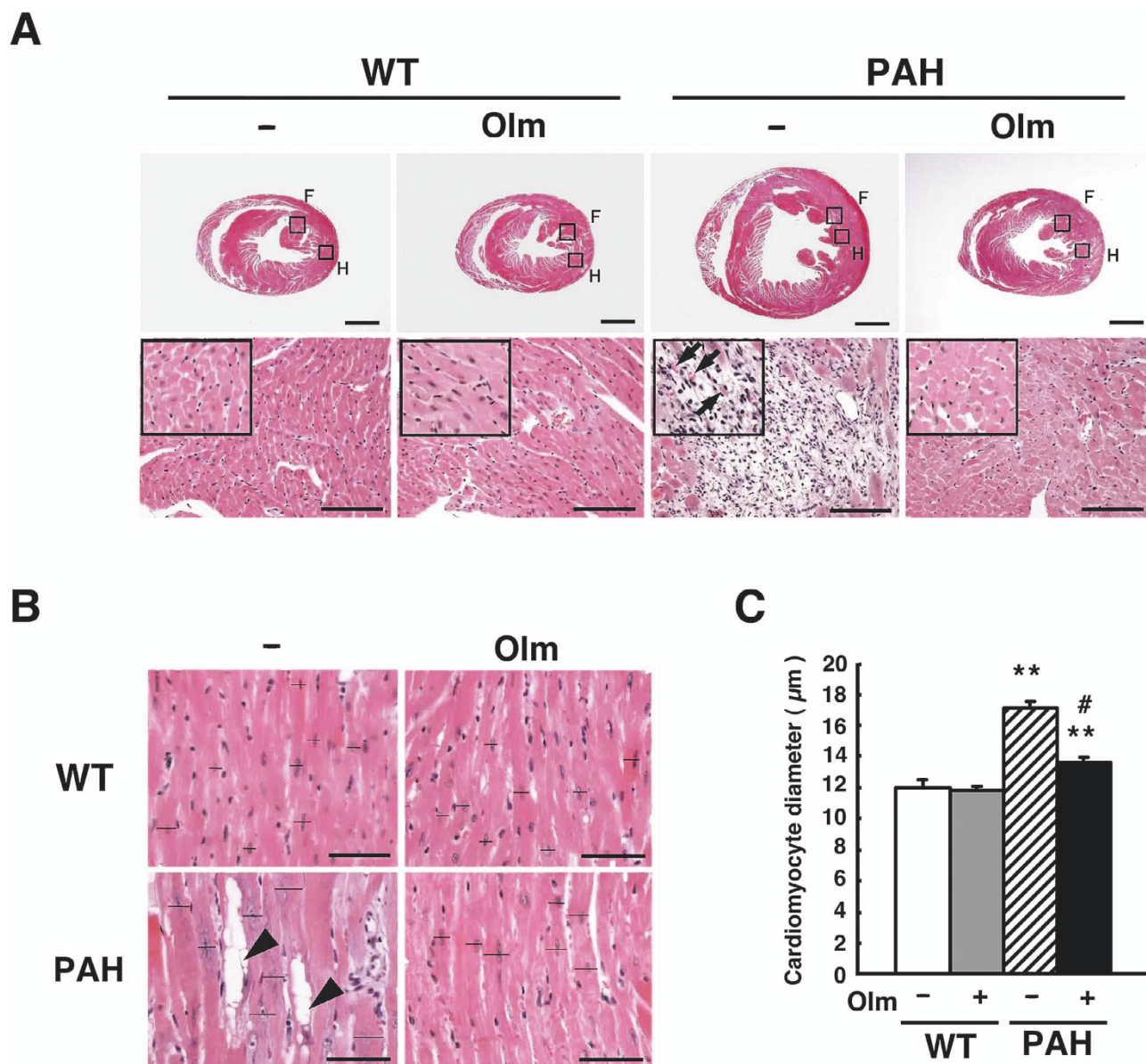


Fig. 3. Histopathological analysis of hearts at 19 d of gestation. *A*: Upper panels show hematoxylin and eosin (H&E) staining of the cross-sectional aspects of the ventricle. Scale bar is 1 mm. Lower panels show higher magnifications of corresponding squares-F shown in the upper panels. Inset indicates a high-power field of the lower panels in each group. A capillary vessel within the granulation tissue in PAH mice is indicated by the arrow. Scale bar is 100 μ m. *B*: Panels show higher magnifications of the ventricle section shown in the corresponding squares-H in the upper panels. Black lines indicate cardiomyocyte diameters in the region of the cellular nucleus. Necrotic cells in the myocardium are indicated by the arrowhead. Scale bar is 50 μ m. *C*: Quantitative determination of myocardial diameters of pregnant mice at 19 d of gestation. ** $p < 0.01$ vs. non-treated WT mice, # $p < 0.01$ vs. non-treated PAH mice.

Prevention of Cardiac Hypertrophy in PAH Mice by Olmesartan Treatment

Gross observation of E19 hearts of PAH mice revealed prominent hypertrophy compared with WT and olmesartan-treated PAH mice (Fig. 2A). The ratio of heart weight to body weight

(HW/BW) of E19 PAH mice was significantly increased compared with WT pregnant mice with or without olmesartan treatment. This elevation of the HW/BW ratio was significantly reduced by olmesartan administration, but HW/BW was still higher than in non-treated or olmesartan-treated WT mice (Fig. 2B). We next measured the plasma levels of CK

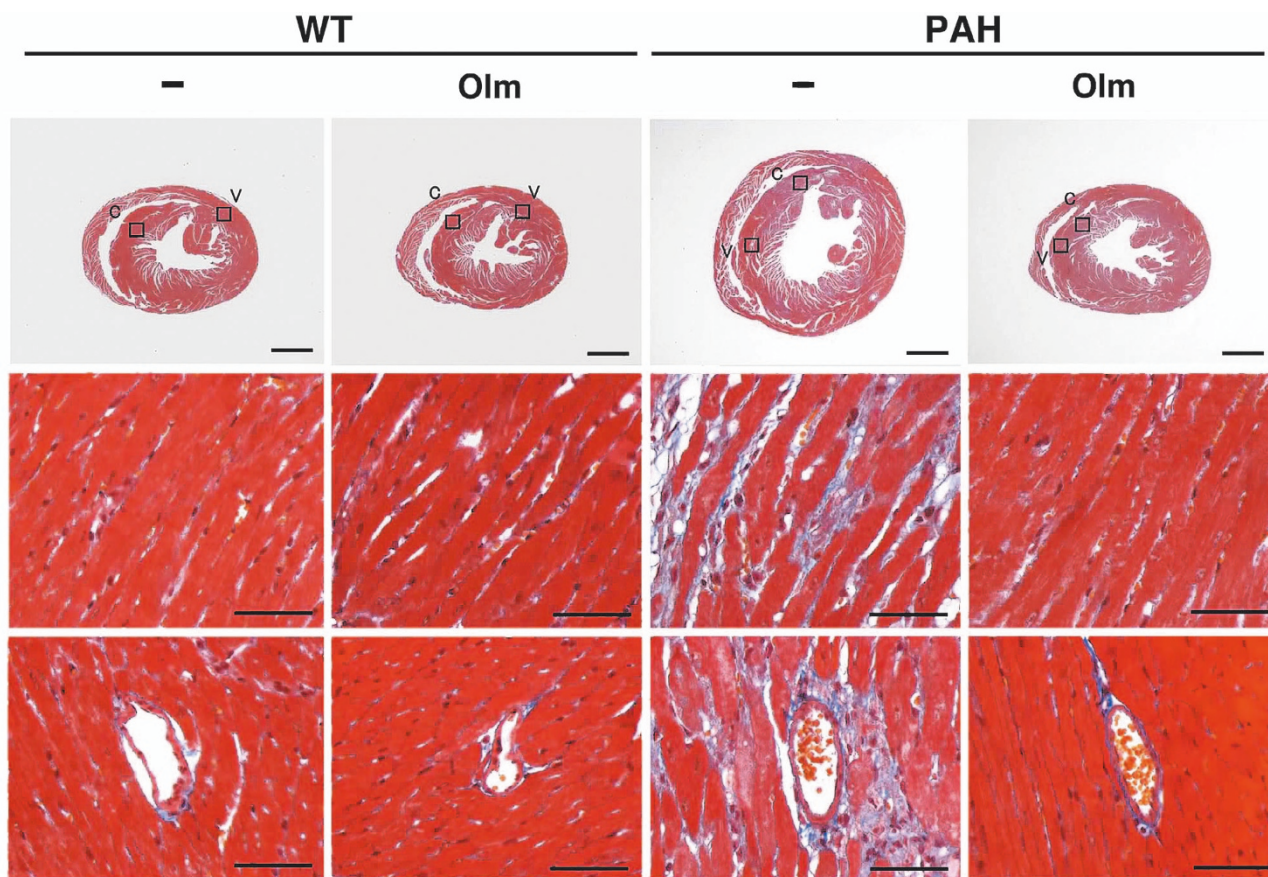


Fig. 4. Histopathological analysis of cardiac fibrosis. Upper panels show Masson's trichrome (MT) staining of the cross-sectional aspects of the ventricle. Scale bar is 1 mm. Middle panels show a higher magnification of cardiomyocytes shown in the corresponding squares-C in the upper panels. Scale bar is 50 μ m. Lower panels show a higher magnification of the intramyocardial blood vessels depicted in the corresponding squares-V in the upper panels. Scale bar is 50 μ m.

and its MB fraction (CKMB), which are molecular makers for cardiac tissue injury. Plasma levels of CK and CKMB in E19 PAH mice were significantly higher than in non-treated and olmesartan-treated WT mice. However, the plasma levels of these markers in olmesartan-treated PAH mice were dramatically reduced to the levels of non-treated and olmesartan-treated WT mice (Fig. 2C, D). These results indicate that AT1 blockade by olmesartan treatment prevents the progression of cardiac hypertrophy and tissue injury in PAH mice.

Effect of Olmesartan on Cardiac Remodeling in PAH Hearts

Increased heart weight with hypertension is often accompanied by cardiac remodeling, including ventricular hypertrophy and fibrosis, which can further aggravate cardiac dysfunction. Therefore, we investigated detailed pathological changes and effects of olmesartan treatment on PAH hearts. Heart sections from E19 PAH mice exhibited considerable hypertrophy compared with sections from non-treated and

olmesartan-treated WT mice (Fig. 3A, upper). In PAH mice treated with olmesartan, ventricular hypertrophy was largely prevented and ventricular morphology appeared to be similar to that of non-treated WT mice. In addition, in PAH hearts, the granulation tissues possessing abundant capillary vessels were diffusely observed in the subendocardial layer of the left ventricle (Fig. 3A, lower, arrows), and necrotic features including vacuoles and hydropic degeneration were also observed (Fig. 3B, arrowheads). Moreover, cardiomyocytes of PAH mice exhibited striking hypertrophy and nuclear swelling compared with non-treated and olmesartan-treated WT mice (Fig. 3B, C). However, in olmesartan-treated PAH mice, granulation tissues and necrotic features in myocardium were not found (Fig. 3B), and the hypertrophy and nuclear swelling of cardiomyocytes were partially alleviated (Fig. 3C).

To further evaluate the effect of olmesartan on cardiac remodeling in PAH mice, we examined cardiac fibrosis using Masson's trichrome staining. Cardiac fibrosis was not observed in non-treated and olmesartan-treated WT mice

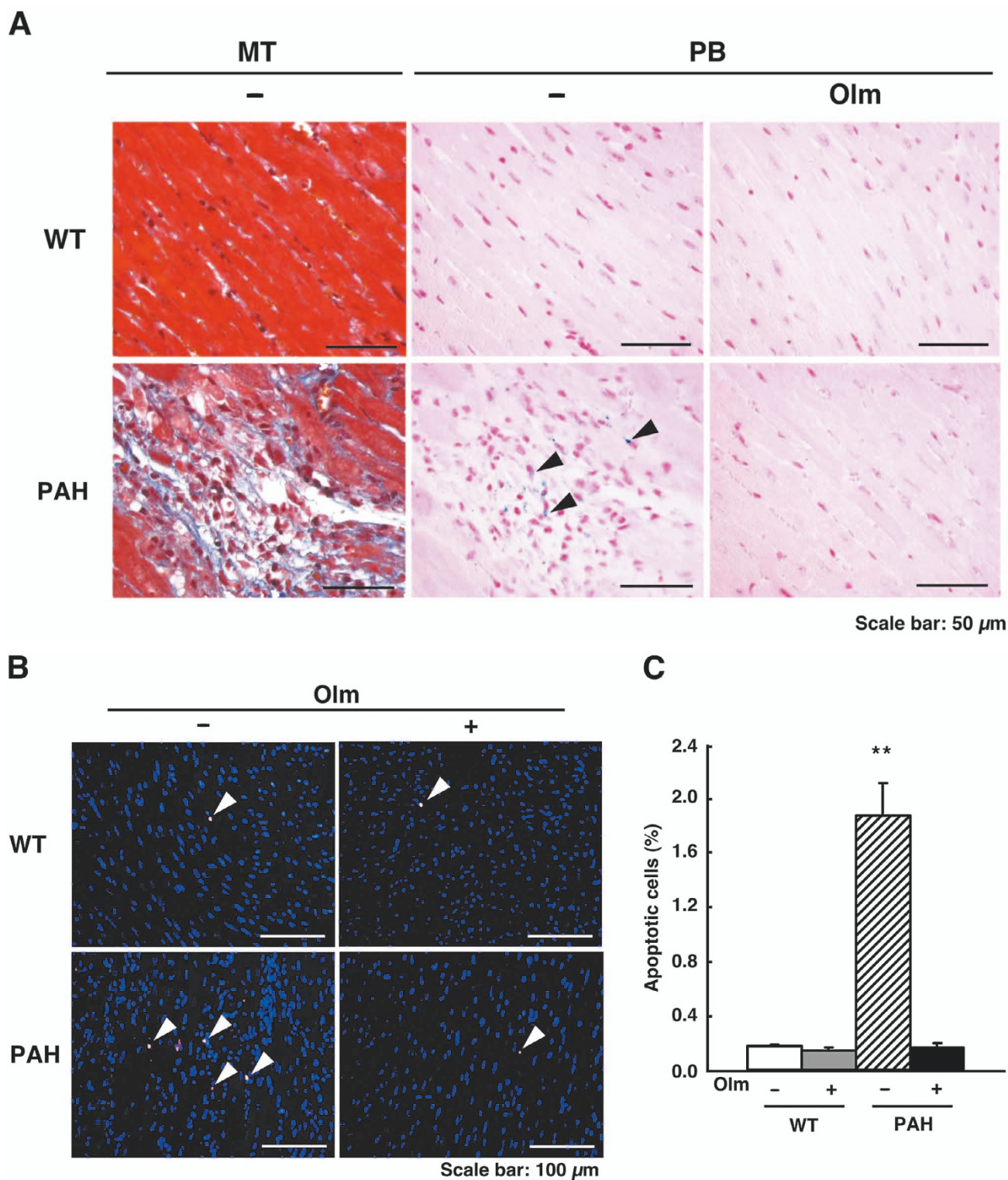


Fig. 5. Prevention of myocardial damage in PAH mice by olmesartan treatment. **A:** Prussian blue (PB) staining of cross-sectional aspects of the ventricle. The iron deposition site in the myocardium is indicated by the arrowhead. Masson's trichrome (MT) staining. Scale bar is 50 μ m. **B:** TUNEL staining of the cross-sectional aspects of the ventricle. TUNEL-positive cells in the myocardium labeled by tetramethylrhodamine (TMR) red are indicated by the white arrowhead. Scale bar is 100 μ m. **C:** Quantitative determination of the percentage of apoptotic cells by dividing the number of TUNEL-positive nuclei by the number of total nuclei. ** $p < 0.001$ vs. non-treated WT mice.

(Fig. 4). However, non-treated PAH mice showed remarkable myocardial and interstitial fibrosis (Fig. 4, middle) as well as fibrosis around large blood vessels (Fig. 4, lower). Myocardial and interstitial fibrosis were apparently prevented by olmesartan administration. These findings indicate that olmesartan prevents cardiac remodeling in PAH mice.

Amelioration of Myocardial Damage in PAH Hearts by Olmesartan Treatment

Cardiac remodeling involves myocardial lesions and apoptosis, resulting in tissue granulation and fibrosis. To further evaluate myocardial damage, we performed Prussian blue staining and found iron deposition and the disruption of cardiomyocytes (24) in E19 hearts. Prussian blue staining did not reveal iron deposition in the hearts of non-treated or olmesartan-treated WT mice. However, at sites of marked cardiac fibrosis in PAH hearts, iron deposition was clearly observed (Fig. 5A, arrowheads); this deposition disappeared after olmesartan treatment. Furthermore, we used TUNEL staining to elucidate the effects of olmesartan treatment on myocardial damage in PAH hearts. The numbers of TUNEL-positive cells were significantly increased in PAH hearts in comparison with non-treated and olmesartan-treated WT hearts (Fig. 5B, white arrowheads), indicating increased apoptosis. The number of apoptotic cells was significantly reduced to the levels of non-treated and olmesartan-treated WT mice by olmesartan treatment (Fig. 5C). These findings indicate that the AT1 blockade by olmesartan prevents myocardial damage and apoptosis in PAH mice.

Discussion

The purpose of this study was to evaluate the effects of AT1 signaling blockade on cardiac remodeling in PIH. Pregnancy is accompanied by important changes in the maternal cardiovascular system. In particular, cardiac dysfunction associated with cardiac remodeling is a serious risk factor for both mother and fetus during PIH (25, 26). Recently, maternal cardiac function was studied in normal and complicated pregnancies with respect to the characterization of systolic and diastolic function, as well as morphological parameters of the left ventricle (27–31). However, little is known about the mechanisms of cardiac remodeling in PIH.

Circulating Ang II levels increase as pregnancy progresses (32) and are thought to play an important role in the establishment of normal pregnancy. The systemic RAS of PIH mothers is not activated, but suppressed (33); thus, RAS was once considered to be unrelated to the pathophysiology of PIH (33, 34). However, the vascular sensitivity for Ang II is elevated in preeclamptic mothers (13). Although the mechanism of increased Ang II sensitivity in PIH long remained unknown, aberrantly activated AT1 signaling was revealed to be a major cause. AbdAlla *et al.* (16) reported that AT1-bradykinin B2 heterodimerization in platelets and omental vessels occurred

more frequently in preeclamptic patients, and they demonstrated that AT1-bradykinin B2 heterodimers facilitate Ang II-induced AT1 signal transduction. In addition, an agonistic autoimmune antibody against AT1 (AT1-AA) was detected in the sera of preeclamptic women; this antibody was associated with maternal and fetal defects in pregnancy (17, 18). These findings suggest that enhanced AT1 signaling in pregnancy contributes to the pathogenesis of PIH. However, the direct relationship between AT1-mediated pathways and the pathophysiological mechanism of preeclampsia remains unknown.

In the PAH mice used in the present study, elevated maternal blood pressure occurs as the result of excess Ang II generation (19–21). Although this marked increase in Ang II is generally not seen in human preeclampsia, facilitated AT1 signaling still appears to play a critical role. Thus, we consider that the PAH mouse model is a useful tool for analysis of PIH. Previously, we detected increased hRN, hANG, and plasma renin activity in the plasma of pregnant PAH/AT1a knockout (KO) mice compared control pregnant mice (20). Surprisingly, however, the blood pressure of PAH/AT1aKO mice was not elevated in late pregnancy despite the presence of AT1b, a subtype of AT1. Maternal and fetal defects such as cardiac and placental abnormalities as well as IUGR observed in PAH mice were not found in PAH/AT1aKO mice. In addition, limited-term administration of AT1 antagonists to PAH mice in late pregnancy dramatically improved their hypertension and IUGR, indicating that activated AT1 signaling pathways play a critical role in the pathogenesis of the PAH model (20). In the current study, we focused on the effects of excess AT1 signaling on cardiac remodeling in PAH mice. Olmesartan administration to PAH dams from E13 resulted in decreased SBP and normalization of weight gain, except for an elevation of blood pressure on E18 and E19 (Fig. 1A). The elevation of blood pressure on E18 and E19 was slight and transient, but not chronic, and the increased weight gain in olmesartan-treated PAH mice was similar to that of non-treated and olmesartan-treated WT mice (Fig. 1B), suggesting that excess AT1 signaling in PAH mice was successfully suppressed.

Cardiac hypertrophy is the major outcome of cardiac remodeling. In addition to pressure overload, activated-AT1 signaling has also been implicated in cardiac hypertrophy both *in vitro* and *in vivo*. Cultured cardiomyocytes stimulated by Ang II become hypertrophic *in vitro*, and this response is inhibited by AT1 antagonists but not by AT2 antagonists (35). In mouse hearts, transgenic over-expression of human AT1 or mouse AT1a also induces cardiac hypertrophy (36, 37). In the present study, cardiac hypertrophy found in PAH mice was prevented by blockade of AT1a pathways (Fig. 2A). AT1b was not detected by RT-PCR in hearts of PAH mice (data not shown); this is consistent with the previous finding that AT1a, but not AT1b, was expressed in the hearts of C57BL/6J mice (38). Therefore, it is likely that AT1a-mediated pathways contribute to cardiac remodeling in PAH mice

because cardiac hypertrophy observed in PAH mice was significantly reduced by suppression of AT1 (Figs. 2B and 3B, C).

In addition to cardiac hypertrophy, cardiac fibrosis is a critical risk factor for cardiac dysfunction accompanied by cardiac remodeling. Cardiac fibrosis is broadly classified into three types: 1) myocardial and interstitial fibrosis, 2) fibrosis around large vasculature, and 3) cardiac scar formation with granulation (39, 40). AT1-mediated signaling is thought to contribute to the development of these types of cardiac fibrosis. Non-myocyte-like fibroblasts in the vicinity of cardiomyocytes stimulated by Ang II become hyperplastic and secrete extracellular matrix components; this response is inhibited by antagonists of AT1 but not AT2 (41–43). Additionally, Ang II-stimulated vascular smooth muscle cells in the heart produce several growth factors and induce auto-hyperplasia and fibroblastic proliferation, resulting in the establishment of fibrosis around the vasculature (44). Cardiomyocyte injury leads to cell death by apoptosis and necrosis, resulting in breakdown of the cardiac structure. To maintain the cardiac structure and function, interstitial and inflammatory cells infiltrate and induce neoangiogenesis, resulting in the formation of the cardiac scar (39, 40, 42, 45). In the current study in PAH hearts, all three types of cardiac fibrosis were present, but dramatically prevented by olmesartan administration (Fig. 4). This result demonstrates a difference between cardiac hypertrophy and fibrosis with respect to olmesartan sensitivity. Interestingly, we observed extensive iron deposition and TUNEL staining in PAH hearts with cardiac scarring; these defects were completely prevented by olmesartan administration (Fig. 5). In addition, AT1 directly activates NADPH-oxidase, enhances the production of oxidative stress, and induces cellular apoptosis (46–49). These reactions probably further exacerbate cardiac injuries in PAH hearts.

Recently, it was reported that levels of soluble fms-like tyrosine kinase-1 (sFlt-1) are elevated in the placenta and serum of women with preeclampsia (50, 51). This factor is thought to be intimately associated with pathogenic aspects of preeclampsia including hypertension, proteinuria, endothelial dysfunction, and IUGR (52, 53). It was also reported that autoantibodies from women with preeclampsia could induce sFlt-1 synthesis and secretion from the placenta through an AT1-mediated pathway (54). In our previous report (22), plasma levels of sFlt-1 were significantly increased in maternal PAH mice at E19 compared with maternal WT mice; this increase might contribute to the pathology of PAH mice. However, the detailed relationship between cardiac remodeling and sFlt-1 in PIH still remains unclear; further study will be required to fully establish this relationship.

In conclusion, our findings provide a new insight into the pathophysiology of cardiac remodeling in pregnancy with hypertension and suggest that treatment with AT1 blockers or other inhibition of aberrant AT1 signaling could effectively ameliorate cardiac dysfunction.

Acknowledgements

We thank Daiichi Sankyo Co., Ltd., Tokyo, Japan for the gift of olmesartan. We are grateful to the members of the Fukamizu Laboratory for their helpful discussions and encouragement.

References

1. National High Blood Pressure Education Program Working Group on High Blood Pressure in Pregnancy: Report of the National High Blood Pressure Education Program Working Group on High Blood Pressure in Pregnancy. *Am J Obstet Gynecol* 2000; **183**: S1–S22.
2. Lavoie JL, Sigmund CD: Minireview: overview of the renin-angiotensin system—an endocrine and paracrine system. *Endocrinology* 2003; **144**: 2179–2183.
3. Paul M, Mehr AP, Kreutz R: Physiology of local renin-angiotensin systems. *Physiol Rev* 2006; **86**: 747–803.
4. Nasjletti A, Masson GMC: Studies on angiotensinogen formation in a liver perfusion system. *Circ Res* 1972; **30**: 187–202.
5. Tewksbury DA: Angiotensinogen-biochemistry and molecular biology. in Laragh JH, Brenner BM (eds): Hypertension: Pathophysiology, Diagnosis and Management. New York, Raven Press, 1990, pp 1197–1216.
6. Chen Y, Naftilan AJ, Oparil S: Androgen-dependent angiotensinogen and renin messenger RNA expression in hypertensive rats. *Hypertension* 1992; **19**: 456–463.
7. Rubattu S, Quimby FW, Sealey JE: Tissue renin and prorenin increase in female cats during the reproductive cycle without commensurate changes in plasma, amniotic or ovarian follicular fluid. *J Hypertens* 1991; **9**: 525–535.
8. Glorioso N, Atlas SA, Laragh JH, et al: Prorenin in high concentrations in human ovarian follicular fluid. *Science* 1986; **233**: 1422–1424.
9. Howard RB, Pucell AG, Bumpus FM, et al: Rat ovarian renin: characterization and changes during the estrous cycle. *Endocrinology* 1988; **123**: 2331–2340.
10. Brown MA, Wang J, Whitworth JA: The renin-angiotensin-aldosterone system in pre-eclampsia. *Clin Exp Hypertens* 1997; **19**: 713–726.
11. Baker PN, Pipkin FB, Symonds EM: Platelet angiotensin II binding and plasma renin concentration, plasma renin substrate and plasma angiotensin II in human pregnancy. *Clin Sci (Lond)* 1990; **79**: 403–408.
12. Baker PN, Pipkin FB, Symonds EM: Comparative study of platelet angiotensin II binding and the angiotensin II sensitivity test as predictors of pregnancy-induced hypertension. *Clin Sci (Lond)* 1992; **83**: 89–95.
13. Gant NF, Daley GL, Chand S, et al: A study of angiotensin II pressor response throughout primigravid pregnancy. *J Clin Invest* 1973; **52**: 2682–2689.
14. Chesley LC, Talledo E, Bohler CS, et al: Vascular reactivity to angiotensin II and norepinephrine in pregnant and nonpregnant women. *Am J Obstet Gynecol* 1965; **91**: 837–842.
15. Crowley SD, Tharaux PL, Audoly LP, et al: Exploring type I angiotensin (AT1) receptor functions through gene targeting. *Acta Physiol Scand* 2004; **181**: 561–570.

16. AbdAlla S, Lothar H, el Massiery A, *et al*: Increased AT₁ receptor heterodimers in preeclampsia mediate enhanced angiotensin II responsiveness. *Nat Med* 2001; **7**: 1003–1009.
17. Wallukat G, Homuth V, Fischer T, *et al*: Patients with preeclampsia develop agonistic autoantibodies against the angiotensin AT₁ receptor. *J Clin Invest* 1999; **103**: 945–952.
18. Zhou CC, Zhang Y, Irani RA, *et al*: Angiotensin receptor agonistic autoantibodies induce pre-eclampsia in pregnant mice. *Nat Med* 2008; **14**: 855–862.
19. Takimoto E, Ishida J, Sugiyama F, *et al*: Hypertension induced in pregnant mice by placental renin and maternal angiotensinogen. *Science* 1996; **274**: 995–998.
20. Saito T, Ishida J, Takimoto-Ohnishi E, *et al*: An essential role for angiotensin II type 1a receptor in pregnancy-associated hypertension with intrauterine growth retardation. *FASEB J* 2004; **18**: 388–390.
21. Takimoto-Ohnishi E, Saito T, Ishida J, *et al*: Differential roles of renin and angiotensinogen in the feto-maternal interface to the development of complications of pregnancy. *Mol Endocrinol* 2005; **19**: 1361–1372.
22. Furuya M, Ishida J, Inaba S, *et al*: Impaired placental neovascularization in mice with pregnancy-associated hypertension. *Lab Invest* 2008; **88**: 416–429.
23. Ishida J, Hashimoto T, Hashimoto Y, *et al*: Regulatory roles for APJ, a seven-transmembrane receptor related to angiotensin-type 1 receptor in blood pressure *in vivo*. *J Biol Chem* 2004; **279**: 26274–26279.
24. Ishizaka N, Saito K, Mitani H, *et al*: Iron overload augments angiotensin II-induced cardiac fibrosis and promotes neointima formation. *Circulation* 2002; **106**: 1840–1846.
25. Garpvic VD, Hayman SR: Hypertension in pregnancy: an emerging risk factor for cardiovascular disease. *Nat Clin Pract Nephrol* 2007; **11**: 613–622.
26. Abboud J, Murad Y, Chen-Scarabelli C, Saravolatz L, Scarabelli TM: Peripartum cardiomyopathy: a comprehensive review. *Int J Cardiol* 2007; **118**: 295–303.
27. Hunter S, Robson SC: Adaptation of the maternal heart in pregnancy. *Br Heart J* 1992; **68**: 540–543.
28. Mesa A, Carlos J, Hernandez A, *et al*: Left ventricular diastolic function in normal human pregnancy. *Circulation* 1999; **9**: 511–517.
29. Valensise H, Novelli GP, Vasapollo B, *et al*: Maternal diastolic dysfunction and left ventricular geometry in gestational hypertension. *Hypertension* 2001; **37**: 1209–1215.
30. Novelli GP, Valensise H, Vasapollo B, *et al*: Left ventricular concentric geometry as a risk factor in gestational hypertension. *Hypertension* 2003; **41**: 469–475.
31. Valensise H, Vasapollo B, Novelli GP, *et al*: Maternal total vascular resistance and concentric geometry: a key to identify uncomplicated gestational hypertension. *BJOG* 2006; **113**: 1044–1052.
32. Zheng J, Bird IM, Chen DB, *et al*: Angiotensin II regulation of ovine fetoplacental artery endothelial functions: interactions with nitric oxide. *J Physiol* 2005; **565**: 59–69.
33. Hanssens M, Keirse MJ, Spitz B, *et al*: Angiotensin II levels in hypertensive and normotensive pregnancies. *Br J Obstet Gynecol* 1991; **98**: 155–161.
34. Kalenga MK, Thomas K, de Gasparo M, *et al*: Determination of renin, angiotensin converting enzyme and angiotensin II levels in human placenta, chorion and amnion from women with pregnancy induced hypertension. *Clin Endocrinol (Oxf)* 1996; **44**: 429–433.
35. Sadoshima J, Izumo S: Molecular characterization of angiotensin II-induced hypertrophy of cardiac myocytes and hyperplasia of cardiac fibroblasts. Critical role of the AT₁ receptor subtype. *Circ Res* 1993; **73**: 413–423.
36. Hein L, Stevens ME, Barsh GS, *et al*: Overexpression of angiotensin AT₁ receptor transgene in the mouse myocardium produces a lethal phenotype associated with myocyte hyperplasia and heart block. *Proc Natl Acad Sci U S A* 1997; **94**: 6391–6396.
37. Paradis P, Dali-Youcef N, Paradis FW, *et al*: Overexpression of angiotensin II type I receptor in cardiomyocytes induces cardiac hypertrophy and remodeling. *Proc Natl Acad Sci U S A* 2000; **97**: 931–936.
38. Kudoh S, Komuro I, Hiroi Y, *et al*: Mechanical stretch induces hypertrophic responses in cardiac myocytes of angiotensin II type 1a receptor knockout mice. *J Biol Chem* 1998; **273**: 24037–24043.
39. Berk BC, Fujiwara K, Lehoux S: ECM remodeling in hypertensive heart disease. *J Clin Invest* 2007; **117**: 568–575.
40. Burstein B, Nattel S: Atrial fibrosis: mechanisms and clinical relevance in atrial fibrillation. *J Am Coll Cardiol* 2008; **51**: 802–809.
41. Crabos M, Roth M, Hahn AW, *et al*: Characterization of angiotensin II receptors in cultured adult rat cardiac fibroblasts. Coupling to signaling systems and gene expression. *J Clin Invest* 1994; **93**: 2372–2378.
42. Harada K, Sugaya T, Murakami K, Yazaki Y, Komuro I: Angiotensin II type 1A receptor knockout mice display less left ventricular remodeling and improved survival after myocardial infarction. *Circulation* 1999; **100**: 2093–2099.
43. Lijnen PJ, Petrov VV, Fagard RH: Angiotensin II-induced stimulation of collagen secretion and production in cardiac fibroblasts is mediated *via* angiotensin II subtype 1 receptors. *J Renin Angiotensin Aldosterone Syst* 2001; **2**: 117–122.
44. Tokuda K, Kai H, Kuwahara F, *et al*: Pressure-independent effects of angiotensin II on hypertensive myocardial fibrosis. *Hypertension* 2004; **43**: 499–503.
45. Kabour A, Henegar JR, Devineni VR, Janicki JS: Prevention of angiotensin II induced myocyte necrosis and coronary vascular damage by lisinopril and losartan in the rat. *Cardiovasc Res* 1995; **29**: 543–548.
46. Nakamura K, Fushimi K, Kouchi H, *et al*: Inhibitory effects of antioxidants on neonatal rat cardiac myocyte hypertrophy induced by tumor necrosis factor-alpha and angiotensin II. *Circulation* 1998; **98**: 794–799.
47. Nishida M, Tanabe S, Maruyama Y, *et al*: G $\alpha_{12/13}$ - and reactive oxygen species-dependent activation of c-Jun NH₂-terminal kinase and p38 mitogen-activated protein kinase by angiotensin receptor stimulation in rat neonatal cardiomyocytes. *J Biol Chem* 2005; **280**: 18434–18441.
48. Skultetyova D, Filipova S, Riecan sky I, *et al*: The role of angiotensin type I receptor in inflammation and endothelial dysfunction. *Recent Patents Cardiovasc Drug Discov* 2007; **2**: 23–27.

49. Schulz R, Heusch G: Angiotensin II in the failing heart. *Kidney Blood Press Res* 2005; **28**: 349–352 (Short Communication).
50. Ohkuchi A, Hirashima C, Matsubara S, et al: Alterations in placental growth factor levels before and after the onset of preeclampsia are more pronounced in women with early onset severe preeclampsia. *Hypertens Res* 2007; **30**: 151–159.
51. Hirashima C, Ohkuchi A, Arai F, et al: Establishing reference values for both total soluble fms-like tyrosine kinase 1 and free placental growth factor in pregnant women. *Hypertens Res* 2005; **28**: 727–732.
52. Maynard SE, Min JY, Merchan J, et al: Excess placental soluble fms-like tyrosine kinase 1 (sFlt1) may contribute to endothelial dysfunction, hypertension, and proteinuria in preeclampsia. *J Clin Invest* 2003; **111**: 649–658.
53. Lu F, Longo M, Tamayo E, et al: The effect of over-expression of sFlt-1 on blood pressure and the occurrence of other manifestations of preeclampsia in unrestrained conscious pregnant mice. *Am J Obstet Gynecol* 2007; **196**: 396.e1–396.e7.
54. Zhou CC, Ahmad S, Mi T, et al: Autoantibody from women with preeclampsia induces soluble Fms-like tyrosine kinase-1 production via angiotensin type 1 receptor and calcineurin/nuclear factor of activated T-cell signaling. *Hypertension* 2008; **51**: 1010–1019.